SENSITIVITY ANALYSIS OF HIGH RESOLUTION GAMMA-RAY DETECTION FOR SAFEGUARDS MONITORING AT NATURAL URANIUM CONVERSION FACILITIES

S. A. Dewji[1,2,*,†], S. Croft[1], N. E. Hertel[1,2]
[1]Oak Ridge National Laboratory, PO Box 2008 MS-6335, Oak Ridge, TN 37831, USA
[2]Georgia Institute of Technology, 770 State Street, Atlanta, GA 30332-0745, USA

Abstract

Under the policies proposed by recent International Atomic Energy Agency (IAEA) circulars and policy papers, implementation of safeguards exists when any purified aqueous uranium solution or uranium oxides suitable for isotopic enrichment or fuel fabrication exists. Under IAEA Policy Paper 18, the starting point for nuclear material under safeguards was reinterpreted, suggesting that purified uranium compounds should be subject to safeguards procedures no later than the first point in the conversion process. In response to this technical need, a combination of simulation models and experimental measurements were employed in previous work to develop and validate gamma-ray nondestructive assay monitoring systems in a natural uranium conversion plant (NUCP). In particular, uranyl nitrate ($UO_2(NO_3)_2$) solution exiting solvent extraction was identified as a key measurement point (KMP). Passive nondestructive assay techniques using high resolution gamma-ray spectroscopy were evaluated to determine their viability as a technical means for drawing safeguards conclusions at NUCPs, and if the IAEA detection requirements of 1 significant quantity (SQ) can be met in a timely manner. Building upon the aforementioned previous validation work on detector sensitivity to varying concentrations of uranyl nitrate via a series of dilution measurements, this work investigates detector response parameter sensitivities to gamma-ray signatures of uranyl nitrate. The full energy peak efficiency of a detection system is dependent upon the sample, geometry, absorption, and intrinsic efficiency parameters. Perturbation of these parameters translates into corresponding variations of the 185.7 keV peak area of the ^{235}U in uranyl nitrate. Such perturbations in the assayed signature impact the quality or versatility of the safeguards conclusions drawn. Given the potentially high throughput of uranyl nitrate in NUCPs, the ability to assay 1 SQ of material requires uncertainty << 1%. Accounting for material self-shielding properties, pipe thickness, and source-detector orientation is instrumental in determining the robustness of gamma-ray detection in the process monitoring of uranyl nitrate in NUCPs. Monte Carlo models and ray-tracing models were employed to determine the sensitivity of the detected 185.7 keV photon to self-shielding properties, pipe thickness, and source-detector geometry. Considering the implementation of the detection of 1 SQ, diversion of 1 SQ becomes essentially undetectable given the systematic uncertainty, in addition to considerations such as propagating uncertainties due to pipe offset/position, as well as minor variations in pipe thickness. Consequently, pipe thickness was the most sensitive variable in affecting full energy efficiency of the 185.7 keV signature peak with up to 8% variation in efficiency for ±0.5 mm changes in Schedule 40 304L stainless steel piping. Furthermore, computation of the attenuation correction factor of the uranyl nitrate solution [CF(AT) (i.e. ε_{sample})] using Parker's method using with the approximation for the geometrical factor $\kappa \approx \pi/4$ was validated through experimental, Monte Carlo and ray-tracing calculations for a uranyl nitrate filled transfer pipe segment. Quantifying sensitivity in detector position, as well as voiding effects due to bubbly flow or laminar flow with an air gap in the uranyl nitrate becomes increasingly important as considerations from (static) design-scale measurements translate into (dynamic) field operations tests.

Keywords: natural uranium, international safeguards, conversion, significant quantity, gamma-ray detection, efficiency, self-attenuation, nondestructive assay, ISOCS, validation, Monte Carlo

---

[*] Corresponding Author: Shaheen Azim Dewji, 1 Bethel Valley Road MS-6335, Oak Ridge, TN, USA 37831-6335, Tel: +1 865 576-9348, E-mail: dewjisa@ornl.gov.

[†] This work was conducted as part of the Ph.D. dissertation of S. Dewji, entitled, "Safeguards Assessment of Gamma-Ray Detection for Process Monitoring at Natural Uranium Conversion Facilities", Georgia Institute of Technology (2014) [1] S.A. Dewji, Safeguards assessment of gamma-ray detection for process monitoring at natural uranium conversion facilities, Nuclear and Radiological Engineering Program, Department of Mechanical Engineering, Georgia Institute of Technology, Atlanta, 2014.

Notice: This manuscript has been authored by UT-Battelle, LLC, under Contract No. DE-AC0500OR22725 with the U.S. Department of Energy. The United States Government retains and the publisher, by accepting the article for publication, acknowledges that the United States Government retains a non-exclusive, paid-up, irrevocable, world-wide license to publish or reproduce the published form of this manuscript, or allow others to do so, for the United States Government purposes. The Department of Energy will provide public access to these results of federally sponsored research in accordance with the DOE Public Access Plan (http://energy.gov/downloads/doe-public-access-plan).

1. INTRODUCTION

Recent circulars and policy papers by the International Atomic Energy Agency (IAEA) have sought to implement safeguards when any purified aqueous uranium solution or uranium oxides suitable for isotopic enrichment or fuel fabrication exists. Motivated by recommendations listed under the IAEA's Policy Paper 18, "Safeguards Measures Applicable in Conversion Plants Processing Natural Uranium" [2], the starting point for nuclear material under safeguards was reinterpreted from Information Circular (INFCIRC) 153 Para. 34(C) under where in the fuel cycle materials are suitable for isotopic enrichment or fuel fabrication exist [3], suggesting that purified uranium compounds should be subject to safeguards procedures no later than the first point in the conversion process.

According to the IAEA, a significant quantity (SQ) is "the approximate amount of nuclear material for which the possibility of manufacturing a nuclear explosive device cannot be excluded. Significant quantities take into account unavoidable losses due to conversion and manufacturing processes and should not be confused with critical masses" [4]. In this scope 1 SQ translates to 10 metric tons of natural uranium over a period of 1 year with a detection probability of 50% [5].

Previous work has focused on validation efforts to determine the capabilities of commercial-off-the-shelf (COTS) gamma-ray detection for safeguards monitoring at the first identified key measurement point (KMP) [6] at natural uranium conversion plants (NUCPs) [7] [8] [9] [10]. A combination of simulation models and experimental measurements were employed to develop and validate concepts of passive gamma-ray detection to monitor solution exiting following solvent extraction the first identified KMP in an NUCP.

In order to determine the ^{235}U mass flow over a detection time period, the validation study by *Dewji et al.* measured the average concentration of uranium in uranyl nitrate solution, from which the ^{235}U weight fraction was measured and determined [10]. The feed uranyl nitrate material is naturally enriched from which the validation study conducted successive dilution experiments to determine the detector's sensitivity to changes in uranium (and hence ^{235}U) concentration. In the following section, these concepts will be developed quantitatively in the context of the experimental mock-up facility and set-ups used. This work employs validated experimental and computational models to determine the sensitivity of the detection [1, 7-10]; the prior validation work was conducted by varying concentrations of uranium content in uranyl nitrate extracted from the Uranyl Nitrate Calibration Loop Equipment (UNCLE) facility at Oak Ridge National Laboratory (ORNL). UNCLE was designed to simulate the full-scale operating conditions of a purified uranium-bearing aqueous stream exiting the solvent extraction process in an NUCP based on the Springfields conversion facility in the United Kingdom. In this prior validation work, a series of static dilution measurements with uranyl nitrate were conducted for uranyl nitrate solution concentrations of 10-90 g U/L [10]. Furthermore, dynamic measurements in the UNCLE test-bed facility were conducted for circulating uranyl nitrate at 500 RPM and 1070 RPM pump speeds [10]. For both static and dynamic measurements, gamma-ray signatures of uranyl nitrate were evaluated; a range of gamma-ray lines was examined, including attenuation for an external source used to evaluate an associated transmission measurement of solution density and uranium concentration.

With spectral data, the ^{235}U concentration can be estimated from a measurement of the ^{235}U 185.7 keV gamma emission once self-attenuation in the solution is accounted for. The self-attenuation correction accounts for the material properties of the uranyl nitrate medium and is based on a transmission (gamma-ray densitometer) technique. A detailed assessment of factors affecting detection efficiency (geometry, attenuation, sample self-attenuation, intrinsic efficiency) is made by conducting a sensitivity analysis of the detector response to changes in pipe thickness, material properties (density/concentration/self-shielding), and source-detector placement/offset. These simulations are conducted using Canberra's In Situ Object Counting System (ISOCS) ray-tracing software [11], as well as validated Monte Carlo models using Monte Carlo N-Particle eXtended (MCNPX) [12].

Interpretation of variation in the detector response affects safeguards interpretations regarding timely detection of 1 SQ.

2. THEORY

Passive gamma-ray detection techniques were employed to assay natural uranyl nitrate at the KMP exiting solvent extraction in an NUCP. In order to assess the sensitivity of high-resolution gamma-ray detection, measurements were conducted with a uranyl nitrate-filled pipe. Static (laboratory) and dynamic (operational) conditions were assessed in the experiments conducted by Dewji *et al.* in Ref. [10]. Variables that contribute to the full energy peak efficiency originate from any of the of following four factors [13]:

$$\varepsilon_{total} = \varepsilon_{geom} \cdot \varepsilon_{absp} \cdot \varepsilon_{sample} \cdot \varepsilon_{int} \tag{1}$$

These four efficiency variables affect the detector response and hence full energy peak efficiency values for the primary 185.7 keV gamma line from ^{235}U decay signature were considered.

- *Sample efficiency (ε_{samp})* quantifies the self-attenuation within the sample material (i.e. the uranyl nitrate in the pipe in the field of view), yielding the fraction of emitted gamma rays that actually emerges from the source (uranyl nitrate) material. This value is the reciprocal of the self-attenuation correction factor, *CF(AT)*, elaborated by Parker's method calculated as a function of transmission values (*T*) [13]:

$$\varepsilon_{\text{absp}} \propto \frac{1}{CF(AT)} = \frac{1-T^{\kappa}}{-\ln(T^{\kappa})}) \tag{2}$$

  where
  κ= geometrical calibration parameter
  (κ <1 for cylindrical samples)
  (κ ≈π/4 for far-field approximation for reasonably transparent cylinders) and
  T= transmission through sample.

  In the scope of this investigation, a combination of measurement data and Monte Carlo simulations were calculated to determine the *CF(AT)* for sample efficiency values for the uranyl nitrate-filled stainless steel pipe.

- *Geometric efficiency (ε_{geom})* is dependent on the solid angle subtended by the source at the detector and can be represented by an inverse square law [13]:

$$\varepsilon_{\text{geom}} \propto \sum_{vol} \frac{1}{R^2} \tag{3}$$

  where R is the point-point source to detector distance. In the scope of this investigation, ray-tracing methods using ISOCS were used to determine the effects of the source-detector distance on the full energy peak efficiency.

- *Absorption efficiency (ε_{absp})* accounts for the effects of intervening materials in the narrow beam geometry case:

$$\varepsilon_{\text{absp}} \propto e^{-\Sigma(\frac{\mu}{\rho})\rho x} \tag{4}$$

  which is dependent on the mass attenuation coefficient (μ/ρ), in addition to density (ρ) and attenuator thickness (x) for the detector housing, shielding, collimators, and sample containers [13]. Exponential attenuation is an energy-dependent parameter. In the scope of this investigation, pipe thickness attenuation is evaluated using ISOCS to determine the effects on the full energy peak efficiency.

- *Intrinsic efficiency* (ε_{int}) is the probability that the gamma ray entering the detector will interact and produce a full-energy peak. The intrinsic efficiency is dependent upon the interaction probability of the detection material and is an inherent property of the detector [13]:

$$\varepsilon_{\text{int}} \propto \varepsilon_{\text{tot}}\left(\frac{peak\ (P)}{total\ (T)}\right) \propto \left(1 - e^{-(\frac{\mu}{\rho})\rho x}\right)\ (\frac{P}{T}) \tag{5}$$

  where (μ/ρ) is the mass attenuation coefficient, (ρ) is density (ρ), and x is the detector thickness.

The intrinsic detection efficiency is not a variable that can be manipulated, so is not tested in the scope of this work. However, the intrinsic efficiency is inherent to all efficiency calculations and spectral analysis as a property of the detector.

Although the sensitivity analysis focuses on static (i.e. not flowing) uranyl nitrate in the 304L pipe, the sensitivity of detector positioning and absorber materials was evaluated. Although many of these variables overlap with variables in dynamic operating conditions, some operational variables differ, e.g. once designed, the ε_{int} remains approximately constant at a given gamma ray energy, but the ε_{absp} could change in the operational facility with uranyl nitrate flowing under dynamic conditions. The best way to quantify these effects would be to conduct the static sensitivity measurements in a field experiment in an operating NUCP. In confining the analysis to static conditions to facilitate measurement feasibility, is prudent to note that voiding effects due to bubbly flow or laminar flow with an air gap in the uranyl nitrate becomes increasingly important as considerations from (static) design-scale measurements translate into (dynamic) field operations tests. In the scope of this study, the sensitivity of variables under static conditions provides detector responses under controlled conditions, which is useful in assessing system design parameters for process monitoring in conversion facilities.

2.1. Properties of Uranyl Nitrate

Static dilution measurements of a uranyl nitrate-filled pipe segment were previously conducted and validated in MCNPX using the Canberra Falcon BEGe detector [10]. The material composition in the pipe segment is described in detail in Ref. [10] and briefly summarized in Table 1. The pipe segment and source uranyl nitrate from the UNCLE facility used in the validation work was modeled based on the Springfields NUCP in the UK, which employs Schedule 40 304L pipe (Table 2) and uranyl nitrate solution circulating which contains 90 g of natural uranium dissolved per liter of water, with a measured solution density of 1.122 g/cm^3 at 20°C.

Table 1. Material Composition of Uranyl Nitrate Solution in Pipe Segment (2.62 L).

Solution Concentration (g U/L)	90	85	75	50	10
Density (g/cm^3)	1.122	1.115	1.099	1.064	1.008
Total Uranyl Nitrate Solution Mass in Pipe (g)	2939.64	2921.30	2879.38	2787.68	2640.96

Table 2. UNCLE Pipe Model Dimensions and Composition.

Component	**Density (g/cm^3)**	**Dimensions (cm)** *diameter × length*
Uranyl Nitrate Solution, 90g U/L (inner	1.122	7.8Ø (inner) × 60.3
Stainless Steel Pipe, 304L	7.9	8.9Ø (outer) × 63.7

The assay was based on the analysis of the 185.7 keV gamma ray peak from ^{235}U in uranyl nitrate, using a high purity germanium detector. Emissions from ^{238}U daughter products were not considered in this study because secular equilibrium could not be assured for freshly solvent extracted uranyl nitrate.[‡]

2.2. Self-Attenuation Correction Principles

Nondestructive assay of uranyl nitrate flowing in NUCP piping presents a geometry configuration that is susceptible to high self-attenuation. To determine the correction factor for self-attenuation, *CF(AT)*, the fraction of the 185.7 keV gamma rays emitted in the direction of the detector that actually reach the detector must be determined.

In order to conduct the calibration, transmission measurements are taken for both the empty and uranyl nitrate-filled pipe. The transmission ratio of the full to empty container is used to determine the sample-specific *CF(AT)* using the method developed by Parker [14], which has previously been employed in NDA field measurements for pipe slurry measurements [15] and for waste-drum assay [16] using high resolution gamma spectroscopy.

Use of transmission calibration provides a reference for assay using transmission techniques to determine the self-attenuation for a sample, in this case, for uranyl nitrate-filled piping. The diametrical transmission, T, through the cylindrical sample is the ratio $T=I/I_o$, where I is the detected count rate of the transmission source energy through the pipe with uranyl nitrate and I_o is the detected count rate through the empty pipe. In this work, a validated MCNP simulation from Ref. [10] was employed to determine the transmission the empty pipe; all photon transport simulations were conducted using MCNPX [12].

For our purposes, T is the predictive variable, Equation 2 provides a convenient functional form, and κ is an empirical parameter that optimally fits the data. In order to conduct the calibration, transmission detection measurements are taken for both the empty and uranyl nitrate-filled pipe. The transmission ratio of the full to empty container is used to determine the sample-specific κ value.

If the sample can be characterized by a linear attenuation coefficient, μ_l, the fraction of photons that detected from the sample can be determined via the following relation:

$$T = e^{-\mu_l \cdot x} \tag{6}$$

Two key assumptions must be satisfied in the scope of this method in order to ensure that the μ_l can sufficiently compute the photon escape-fraction on a macroscopic scale [14]: (i) the gamma-ray source material (i.e., uranyl nitrate solution) is reasonably homogeneous in composition, and (ii), the gamma-ray emitting constituents are small enough such that self-attenuation within the individual particles (i.e., uranium) is negligible.

In the validation work by Dewji *et al.*, a 1-D demonstration of the effects of the relative *CF(AT),* based on calibration with 90 g U/L uranyl nitrate for the 185.7 keV gamma ray from ^{235}U, with a relative transmission of the 122 keV from ^{57}Co was conducted [10]. A detailed, 3-D model of *CF(AT)* of the uranyl nitrate pipe segment is presented in more detail here, using the experimental validation data and ISOCS simulations.

3. METHODS

[‡] The scope of this project assumes that secular equilibrium cannot be ensured, hence focusing on the direct ^{235}U-based assay signatures, though the other lines are available to measure experimentally in this special situation to add complementary information. The difference between recently purified and aged uranyl nitrate for ^{235}U activity is negligible ($< 4\times10^{-6}$ %), given the long half-life of ^{235}U; thus, we can assume the activity at 44 years (as in UNCLE) for ^{235}U approximates the response from recently purified ^{235}U.

A detailed assessment of factors affecting detection efficiency is made by conducting a sensitivity analysis of the detector response to changes in pipe thickness, material properties, and source-detector placement/offset. Since all geometry and material composition variables could not be experimentally tested, computational models were constructed to simulate the detector responses.

Ray-tracing calculations were employed using Canberra's ISOCS software [11]. Unlike classical efficiency calibrations, ISOCS can be employed without having to use radioactive source standards. The response of the specific HPGe detector has been previously characterized by the manufacturer using mathematical methods. The geometry is modeled in the ISOCS software, which uses ray tracing to determine the peak efficiency of the 3-D source-detector system. When this efficiency calibration is applied to an acquired spectrum, the mass (and hence, activity) can be determined for the modeled geometry. The use of ISOCS obviates having to run multiple MCNPX simulations, hence permitting testing of a multitude of variables affecting the overall peak efficiency of photon signatures using the ISOCS Uncertainty Estimator (IUE) tool.

In ISOCS, the modeled uranyl nitrate comprises of solutions ranging from 10-90 grams of uranium dissolved per 1000 mL of water, 0.76% enrichment, with a measured solution densities of 1.008-1.122 g/cm^3. For the stock uranyl nitrate solution at 90 g U/L, elemental solution composition was calculated to be 8.0 wt.% U, 0.70% N, 81.5% O, and 9.8% H.

3.1. In Situ Object Counting System (ISOCS)

Models were created to emulate the geometry employed for both the dilution and UNCLE measurements from Ref. [10]. The uranyl nitrate composition from Table 1 and pipe dimensions from Ref. [10] were employed in the ISOCS models. The ISOCS model of the Falcon BEGe included a tungsten (W) collimator, where the endcap modeled as an epoxy absorber to best simulate the Falcon's collimator composition, as shown in Figure 1 [17].

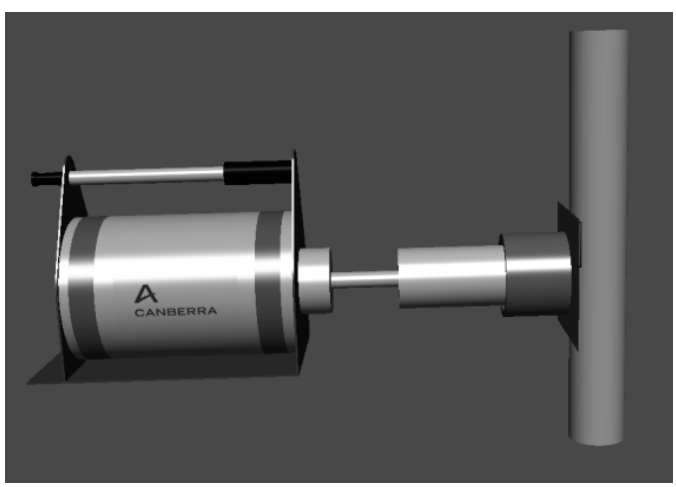

Figure 1. ISOCS model of a Pipe measured using a Falcon BEGe with collimator.

When the ISOCS based efficiency calibration is applied to an acquired spectrum, the activity (and hence the mass) can be determined for the modeled geometry. This calibration is conducted over 0 mm to 500 m distance in all directions of the detector, over an energy range of 45 keV - 7000 keV [11]. ISOCS executes in a short time relative to MCNP, but generates only the full energy peak efficiency, not the energy deposition profile.

In the scope of this sensitivity analysis, ISOCS was employed to determine: (1) Validation of total full energy peak efficiency (ε_{total}); (2) Change in efficiency due to variations in thickness in pipe boundary interface (ε_{absp}); (3) Change in efficiency due to variations in detector offset and axial source-detector distance or horizontal detector offset (ε_{geom}); and (4) Sample efficiency (self-attenuation) and variation in concentration from 10-90 g U/L (ε_{samp}).

4. RESULTS

Evaluation of each of these parameters to the overall detector response determined the sensitivity of a passive gamma-ray system for safeguards monitoring at an NUCP based on the 185.7 keV signature.

4.1. Peak Efficiency Calculations (ε_{total})

Models were created to emulate the geometry employed for both the dilution (static) and UNCLE (dynamic) measurements. The peak efficiency values determined using ISOCS were calculated within 1% convergence error. The results for the Falcon BEGe are provided in Figure 2 and are plot as a function solution density for the 185.7 keV peak efficiency in Figure 3. All data are plotted with 1% error bars. One prominent feature of these simulations is the efficiency drop above 100 keV. This local drop in efficiency is due to the K-edge absorption of uranium at 115.6 keV. At lower uranium concentrations, the relative K-edge effect is less pronounced.

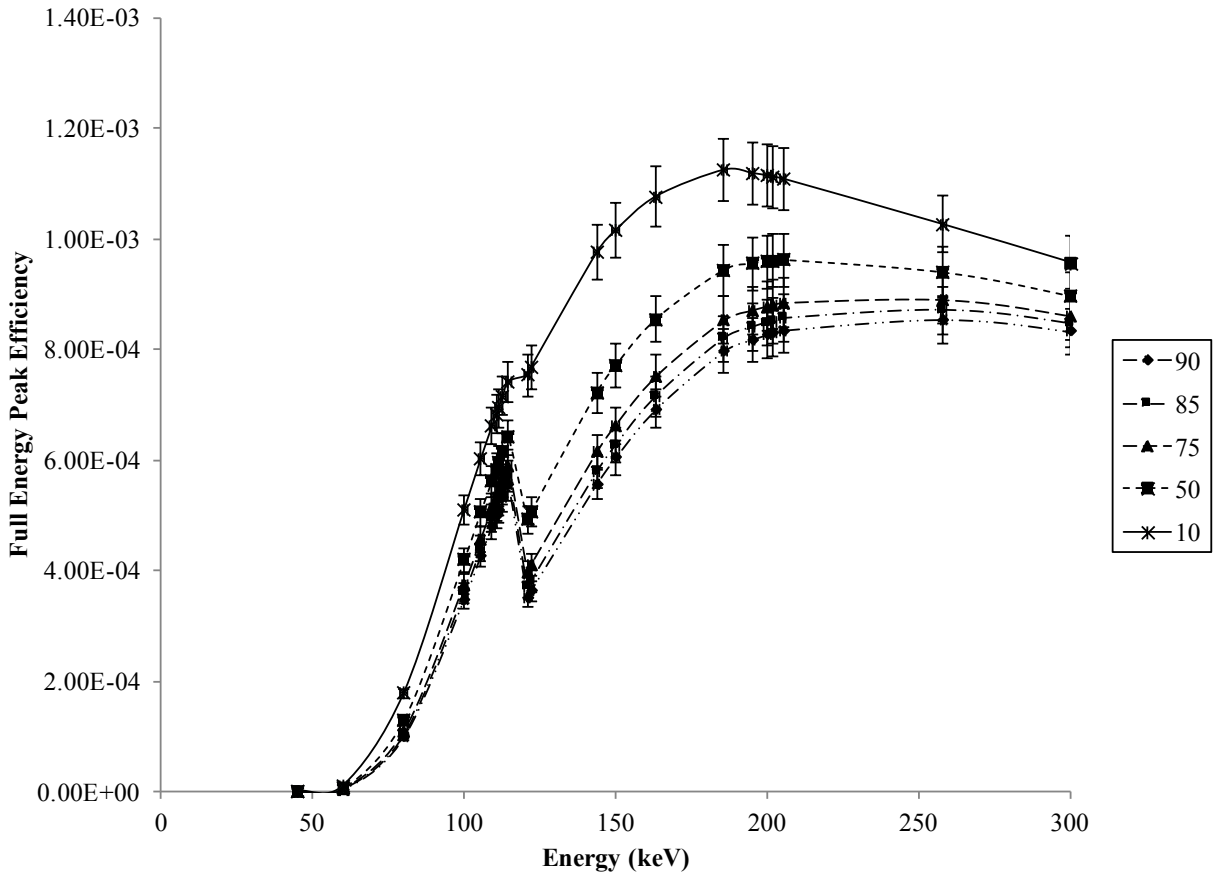

Figure 2. ISOCS Calculated Peak Efficiencies for Collimated Falcon at Dilution Concentrations as a Function of Energy.

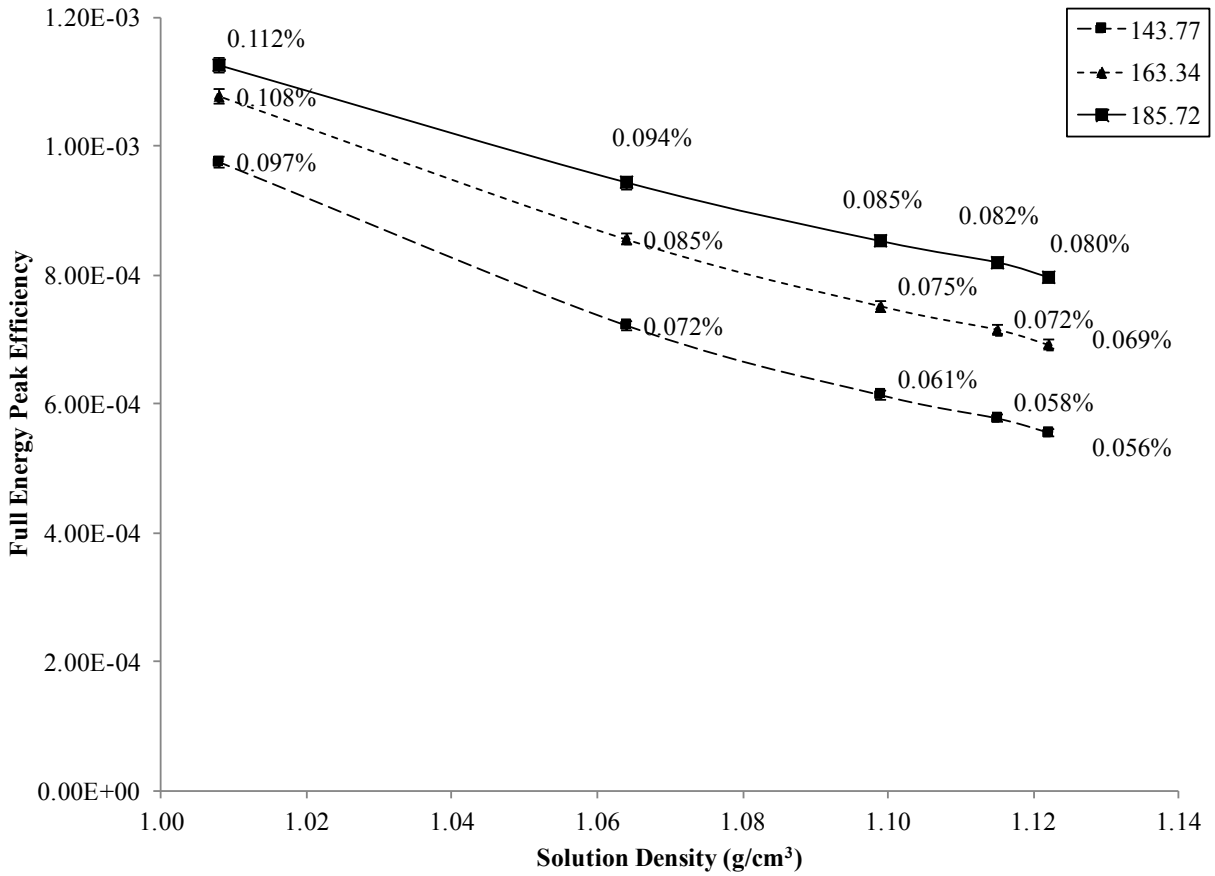

Figure 3. ISOCS efficiency calculations for collimated Falcon measurements as a function of uranyl nitrate solution density.

4.1.1. Mass and Activity Calculation of Uranyl Nitrate in Static and Dynamic Experiments

With a branching ratio of 0.572 for 185.7 keV photons per decay [18], and knowing the ^{235}U specific activity of 7.84×10^{4} photons/s/g calculated from ISOCS, peak area can be correlated with ^{235}U mass as shown in Equation 8.

$$^{235}U\ Mass = \frac{^{235}U\ Activity\ (Bq)}{^{235}U\ Specific\ Activity\ (photons/s/g)}\ . \tag{8}$$

Modeling the source-detector setup enables ISOCS to generate the geometry-specific peak efficiencies. These efficiency calibrations were imported into the dilution data taken with the Genie spectral analysis software [19] for the Falcon detector. With ISOCS-generated peak efficiencies, the mass and subsequent activity of ^{235}U were determined for the dilution setup, and summarized in Tables 1 and 2.

Theoretical ^{235}U mass values were calculated using stoichiometric calculations and measured densities for the uranyl nitrate-filled pipe. Table 4 summarizes the same generated ISOCS efficiency for the flowing 90 g U/L solution from the UNCLE spectra taken with the Falcon detector. Consistent with the peak area results discussed in Ref. [10], a lower effective mass is seen by the detector due to dynamic flow (i.e. caused by void fraction due to turbulent flow introduced by the pumps), as well as any variations in the exact geometry setup from the dilution measurements translated to UNCLE. As seen with the dynamic flow measurements, it is possible that higher void fraction from higher rpm causes the overestimate bias, which warrants further investigation.

Table 3. ISOCS Mass and Activity of Uranyl Nitrate in Static Dilution Pipe from Falcon BEGe.

Dilution Concentration (g U/L)	Theoretical Calculation Mass ^{235}U in Pipe (g)	ISOCS Falcon BEGe Mass ^{235}U in Pipe (g)	ISOCS BEGe Specific Activity ^{235}U (photons/s/g)
90	1.99	1.85± 0.05	7.84×10^4
85	1.87	1.79± 0.04	7.83×10^4
75	1.66	1.62± 0.04	7.86×10^4
50	1.10	1.09±0.02	7.81×10^4
10	0.22	0.17±0.01	7.84×10^4

Table 4. ISOCS Mass and Activity of Uranyl Nitrate in Dynamic UNCLE from Falcon BEGe.

	ISOCS Mass ^{235}U (g)	ISOCS Falcon Specific Activity ^{235}U (photons/s/g)
Theoretical	1.99	8.00×10^4
BEGe Dilution 90g U/L [10]	1.85± 0.05	7.84×10^4
BEGe UNCLE 1070 RPM [10]	1.73± 0.04	7.83×10^4
BEGe UNCLE 500 RPM [10]	1.66± 0.04	7.83×10^4

The 185.7 keV peak area can be written as a function of source activity and efficiency variables for uranyl nitrate, given in Equation 9.

$$185.7keV\ Peak\ Area\ (cps)\ = {}^{235}U\ Activity\ (Bq) \cdot \varepsilon_{peak\ {}^{235}U} \cdot Y_\gamma \qquad (9)$$

The Falcon static measurement data yielded a 185.7 keV peak efficiency (ε_{peak} *of* $^{235}U \equiv \varepsilon_{total}$ in Equation 9) in ISOCS of (0.073±0.001)%, where the ISOCS theoretical model yielded (0.080±0.004. Y_γ is the gamma ray yield (or gammas per decay) of the 185.7 keV gamma emission.

4.2. Sample Properties Peak Efficiency (ε_{samp})

In determining *CF(AT)* in the scope of this work, *T* was calculated by taking a transmission ratio of the uranyl nitrate-filled pipe *(I)* with an empty pipe *(Io)*. The signal measured was from BEGe detector measurements of the ^{137}Cs 661.7 keV transmission signal. As discussed in detail in Ref. [10], ^{137}Cs was selected due to source availability during the measurement campaign, but was determined to be sub-optimal for uranyl nitrate densitometry. As empty pipe measurements were not feasible in this experimental work, a Monte Carlo model was developed and validated based on acquired measurements. The ratio of *I/Io* is related to *T* through the inner diameter of the pipe, *d,* via the relation given in Equation 6. Transmission measurements were conducted using the 661.7 keV emission from 137Cs and scaled to determine the *CF(AT)* for the 185.7 keV from ^{235}U using Parker's method.

The net peak area of the transmitted 661.7 keV photons through the full and empty pipes provided a value for *T*. Applying Equation 6 to the validated transmission simulations provides *T* for each of the dilution densities/concentrations. The plot of *ln(1/T)* as a function of solution density (for each dilution concentration) is shown in Figure 4.

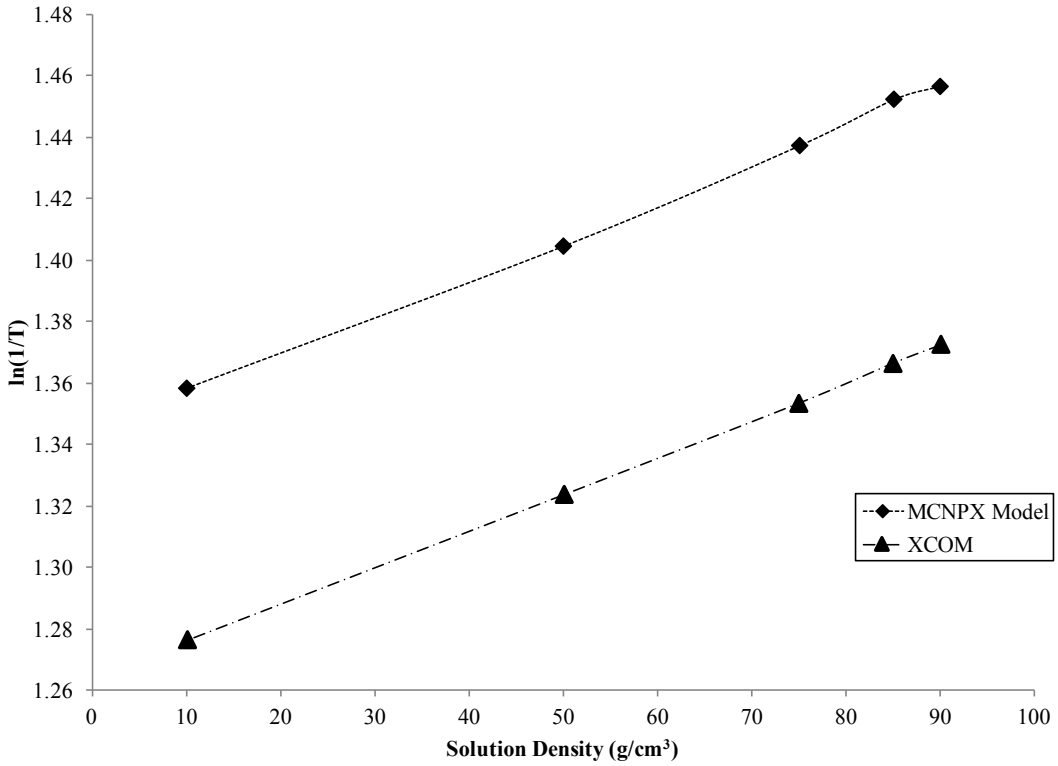

Figure 4. ^{137}Cs Source Transmission as a Function of uranyl nitrate solution density for calculation of *CF(AT).*

Note that in Figure 4, the transmission measurements were compared to the transmission values calculated in the previous section with NIST XCOM attenuation coefficients for narrow-beam geometry [20]. The transmission value *(T)* is determined in 2 ways: (i) using Beer's law and NIST XCOM values for mass attenuation coefficient, and (ii) using ^{137}Cs transmission source. The correction factor *(CF)* using Parker formalism is then calculated using the two different transmission values. The Parker method employed to determine the *CF* is common; the method to determine *T* is different. Taking into account source-detector geometry and self-attention of the material results in a lower transmission value, which is consistent with the results of Figure 4.

Finally, applying Equation 2 for various values of κ (empirically determined) to the ^{137}Cs transmission data provides us the overall calculation of *CF(AT)* for our UN-filled pipe, given in Figure 5. Figure 6 provides an alternative view of *CF(AT)* as a function of transmission through UN of each of the dilution concentrations. Figure 5 and Figure 6 are consistent with the similar experiment conducted by Parker [21].

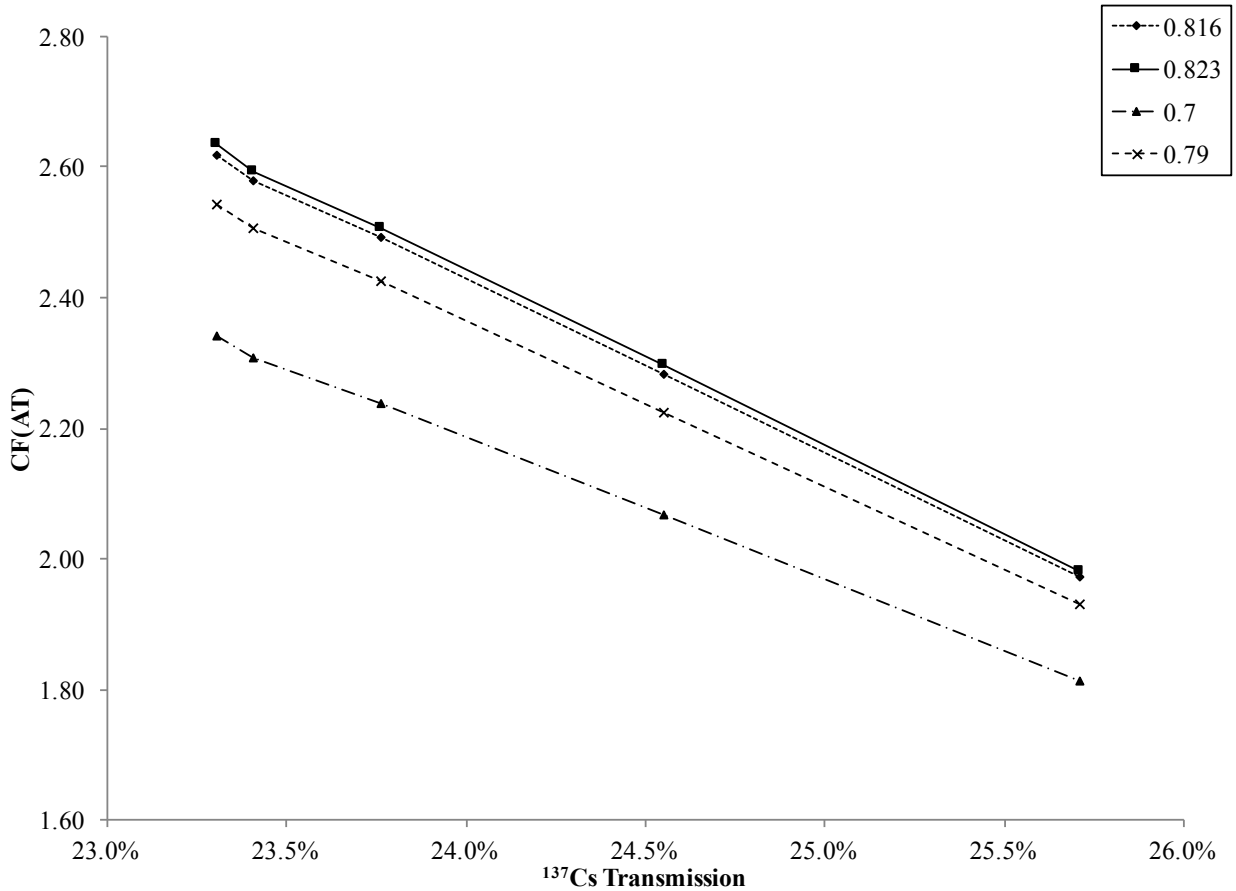

Figure 5. Calculation of *CF(AT)* for uranyl nitrate-filled pipe as a function of transmission through dilution concentrations using Equation 2 for values of *κ* (0.7-0.823, in legend).

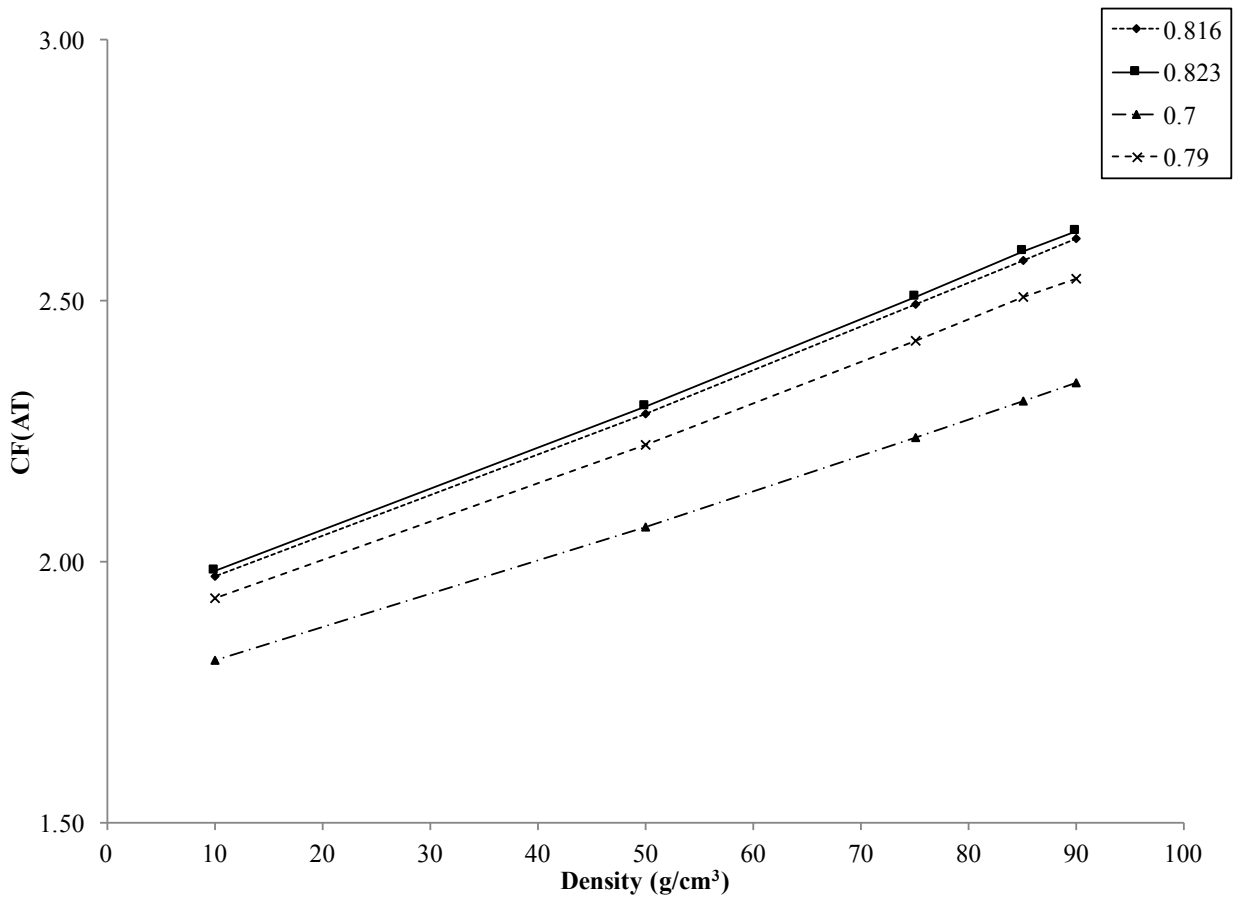

Figure 6. Calculation of *CF(AT)* for uranyl nitrate-filled pipe as a function of dilution concentrations using Equation 2 for values of κ (0.7-0.823, in legend).

4.3. Absorber Sensitivity (ε_{absp})

The following ISOCS models build upon characterizing the ε_{total} by determining the effects of removing the collimator/shielding. Since the Falcon is modeled with the integral W collimator endcap and Pb brick arrangement, the uncollimated/unshielded models without 304L piping enable direct comparison of the variables contributing to ε_{total} independent of ε_{absp}.

ISOCS models were constructed without the 304L pipe wall (modeled as dry air). Figure 7 shows a comparison of efficiencies calculated by ISOCS for the Falcon with 90 g U/L uranyl nitrate in for various shielding and absorber geometries. These geometries are a variation of calculated efficiencies with and without the 304L pipe wall and/or collimator. Figure 7 demonstrates the effect of each of these absorbers, which lends to later discussion on how varying pipe thickness could be used for spoofing, or how uncertainties in pipe thicknesses lead to altered conclusions of materials throughput (and hence MUF). All efficiencies were calculated by ISOCS within 5% uncertainty, which is present in ISOCS as the default for this energy range in the analysis software code.

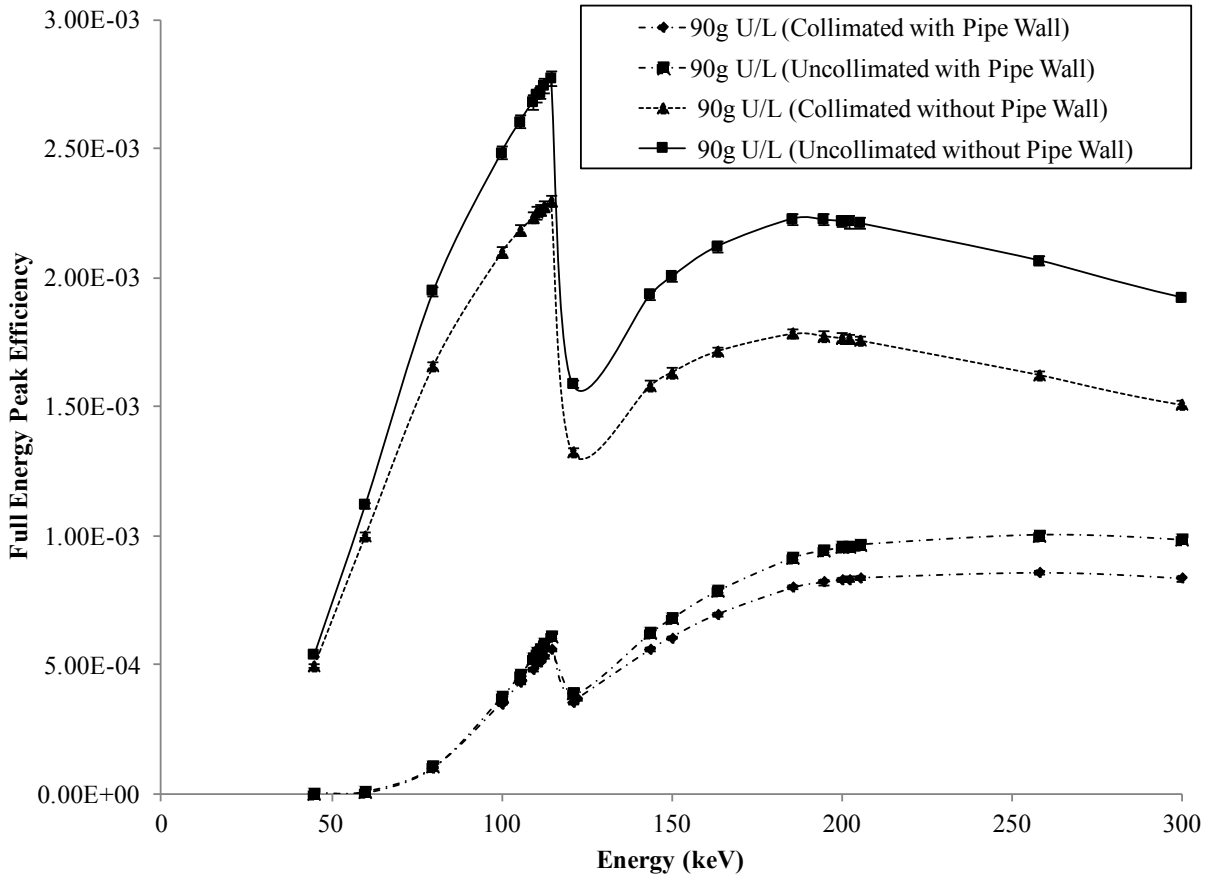

Figure 7. Comparison of ISOCS Efficiency Calculations of 90 g U/L Uranyl Nitrate for Falcon BEGe (i) with Pipe and Collimation; (ii) with Pipe Wall Without Collimation; (iii) with Pipe with Collimation; and (iv) without Pipe or Collimation.

At 185.7 keV, the peak efficiencies generated by ISOCS for these various geometries are summarized in Table 5.

Table 5. ISOCS 185.7 keV Peak Efficiencies for Various Geometries.

Geometry	Falcon Peak Efficiency
Collimated, Pipe Wall	0.080%
Uncollimated, Pipe Wall	0.091%
Collimated, No Pipe Wall	0.178%
Uncollimated, No Pipe Wall	0.223%

For the Falcon at 90g U/L, the peak efficiency for a collimated detector with pipe wall is 0.080%. The presence of the pipe wall attenuates the source uranyl nitrate by 59.2%. The ISOCS simulation demonstrates that the presence of the W collimator attenuates 12.1% of the incident 185.7 keV photons. As a result, the contribution to ε_{absp} for the Falcon at 90g U/L can be calculated as the quotient of the efficiency with shielding/collimation/piping with the efficiency without these absorbers. The result for the Falcon is a 35.8% contribution to ε_{absp}, due to pipe wall and collimator effects.

Analysis of the attenuation effects of the source and detector system provides essential insights into the characteristics of the uranyl nitrate material flowing in NUCPs. Identification of the photon interactions occurring provided an assessment of the behavior of the 185.7 keV photons as a monitoring signature. Furthermore, attenuation analysis provided a basis for identifying which external densitometry transmission sources were optimal for monitoring density and uranium content. Although the ^{57}Co was preferable to ^{235}U transmission measurements, the availability of ^{137}Cs suffices for determining the correction factor due to self-attenuation of the UN-bearing pipe [10]. Determination of the correction factor due to self-attenuation provided a source-detector geometry-corrected assessment of what fraction of emitted ^{235}U gamma rays actually reached the detector. As expected, narrow-beam geometry theoretically predicted higher transmission values in the absence of accounting for self-attenuation.

A variety of methods have been employed to determine the peak efficiency of the 185.7 keV emission, including efficiency calculations from MCNPX, measurement data, and ISOCS simulations. Determination of the ε_{sample} provides the *CF(AT)* as outlined by Parker's method. The inverse value of this efficiency yields a *CF(AT)* of 2.49±0.02. Using Parker's method in combination with the MCNPX transmission model employed in Ref. [10], *CF(AT)* was plotted as a function of κ. From the calculated ε_{sample}, the κ in Equation 2 can be determined from the *CF(AT)* for the Falcon. Figure 8 shows *CF(AT)* as a function of κ for XCOM, dilution data [1] [10], and UNCLE [1] [10]. Since *CF(AT)* was determined to be 2.49, the subsequent values for κ (based on dilution data) are provided in Table 6, where κ ~0.75–0.76. Thus, κ is well approximated by the estimate of $\pi/4$ for a cylinder [21].

Beer's law (XCOM) is overstated as it theoretically predicts *CF(AT)* for narrow-beam geometry. Variations in reproducible geometry between the dilution and UNCLE measurements explain the difference in κ [10]. These factors are adequately determined and confirmed for design purpose, which can be experimentally determined for any final instrument prior to entering into service.

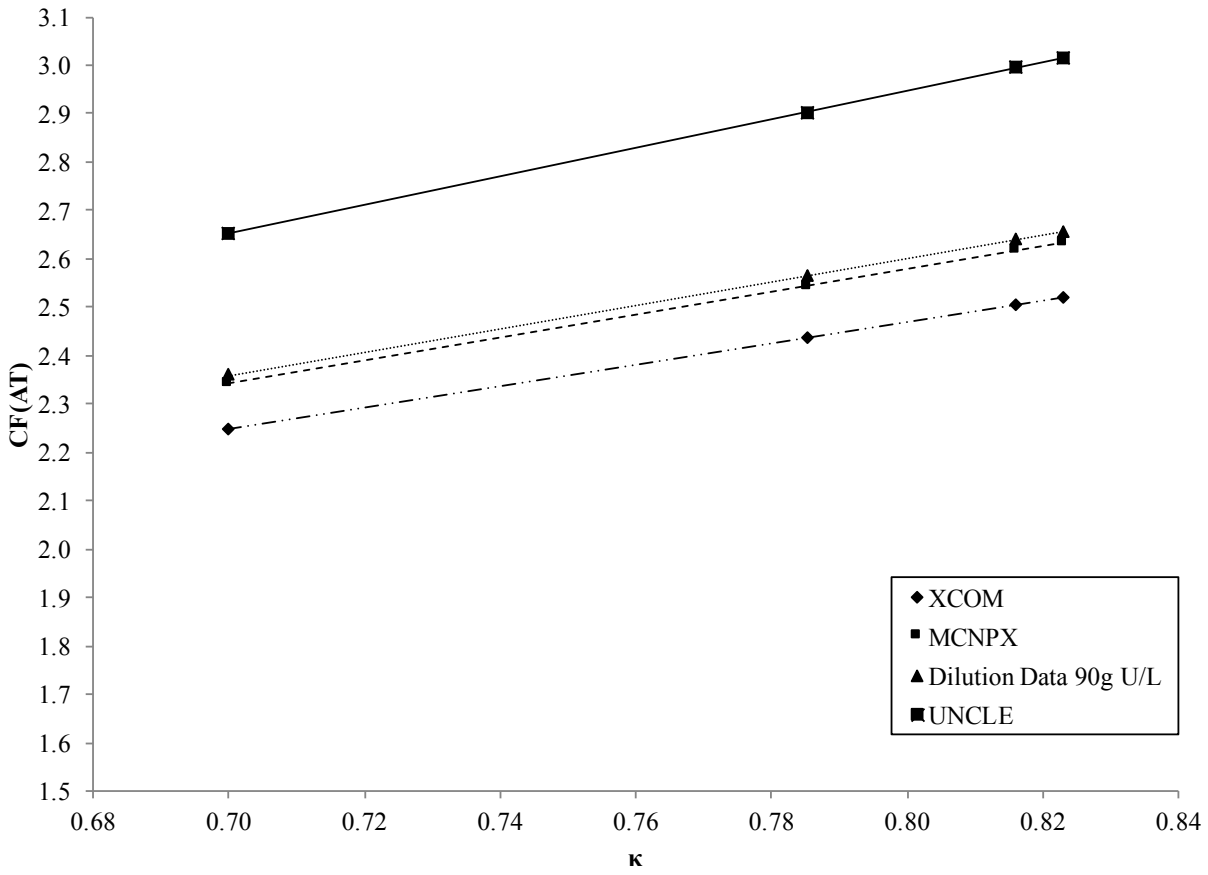

Figure 8. Calculation of *CF(AT)* for Various Values of *κ* (Equation 2) .

Table 6. Calculation of κ Based on Derived Values of *CF(AT)*.

CF(AT)	XCOM	Dilution Data 90 g U/L	UNCLE
2.49	0.81±0.01	0.75±0.01	0.65±0.01

4.4. Detector Position Sensitivity (ε_{geom})

The use of simulation tools, such as ISOCS, permit testing the sensitivity of detector responses to how geometric and absorber variables such as source-detector geometry and pipe thickness, respectively, affect the overall detection efficiency of the assayed ^{235}U signatures.

4.4.1. Detector Offset

The ISOCS Uncertainty Estimator was employed to calculate the 185.7 keV peak efficiencies at discrete offset locations ranging from 0 to 25 cm. The offset position represents the movement of the detector face perpendicular to the axial length of the pipe segment. Models were created to simulate the Falcon with W collimator, as described in the previous section for the efficiency calculation simulations. Figure 9 shows the results of the peak efficiencies from high-intensity ^{235}U signatures from 0 to 25 cm offset values for the Falcon. The 185.7 keV emission was empirically fit to determine the peak efficiencies at 0 cm, 6.5 cm and 13 cm; these efficiency values are summarized in Table 7.

Table 7.

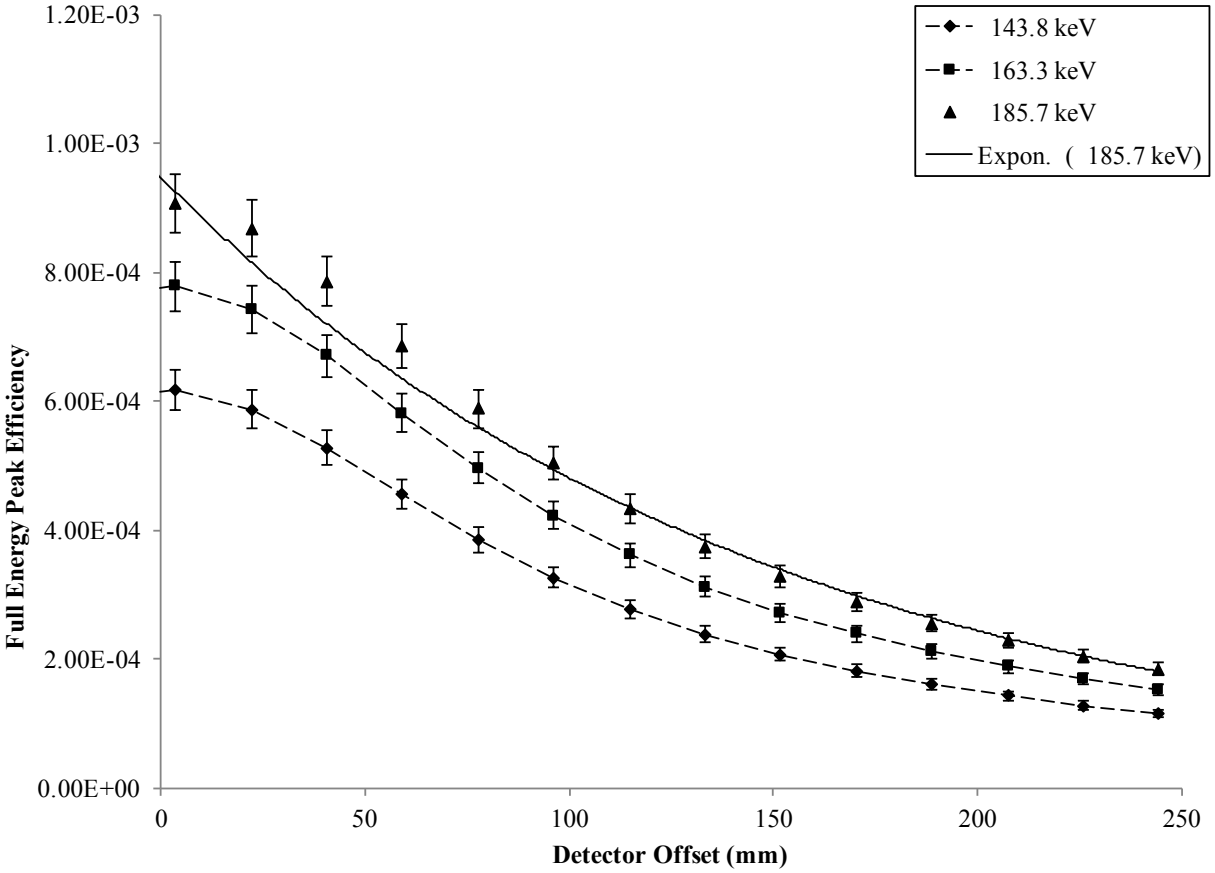

Figure 9. ISOCS Uncertainty Estimator Simulations: Efficiency Calculations for Falcon Detector at Various Distances from Source along Central Axis.

For the 185.7 keV peak efficiency to drop to 50% of its initial value, the Falcon must be offset by 9.9 cm, making the position sensitivity in the Falcon in field operating conditions of interest given the detector could be subject to vibration and thermal expansion of the uranyl nitrate-filled pipe, given the demands of a field operating environment.

Table 7. ISOCS Peak Efficiency Results for Falcon and Osprey Detectors at Measurement Offset Locations.

Offset (cm)	Falcon 185.7 keV Full Energy Peak Efficiency
0	0.090%
6.5	0.057%
13	0.036%

The ISOCS Uncertainty Estimator calculates the efficiency associated with displacing the pipe at set offset distances for the modeled geometry. However, unlike the experimental measurements, ISOCS cannot predict added background effects in an operational environment that may originate from adjacent pipes and tanks in an NUCP. Background additionally increases the continuum under the peak area. In reality, this can be remedied by an optimized shielding design that encapsulates the pipe and detector to prevent gross displacements between the source and detector, in addition to shielding leakage from background.

4.4.2. Source-Detector Distance

Varying the source-detector distance along the central axis was simulated using the Uncertainty Estimator for values up to 120 cm (Figure 10). Although a transfer pipe in a conversion facility could be assumed to be infinitely long, the effect of detector position was employed here as part of the comprehensive sensitivity analysis. Depending on field conditions, it may be conceivable that the detector could best be affixed on a shorter segment transfer pipe, for which this sensitivity model informs such a prospect.

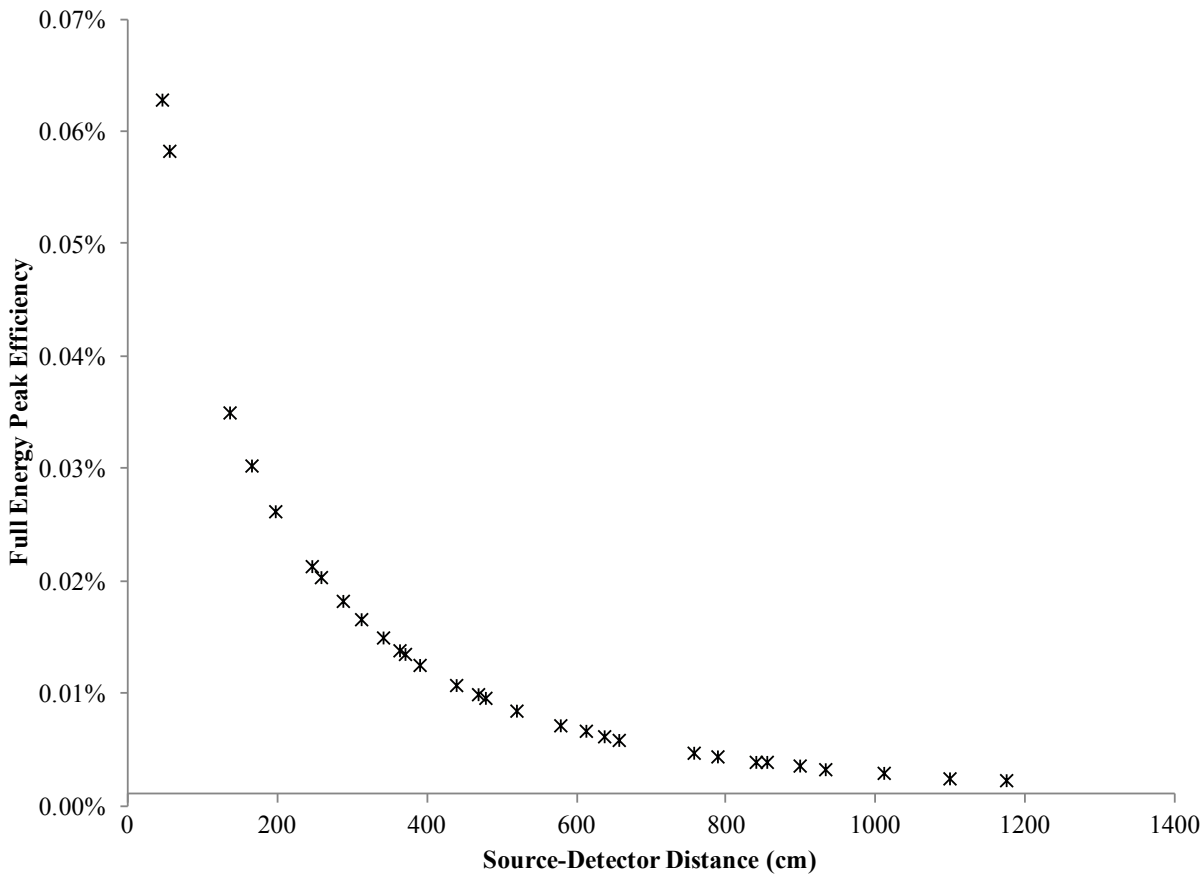

Figure 10. ISOCS Uncertainty Estimator Simulations: Efficiency Calculations for Falcon Detector at Various Distances from Source along Central Axis for 185.7 keV Emissions.

As with the offset simulations, ISOCS Uncertainty Estimator provides an estimate without consideration to other operational background. Moving the detector further from the pipe would increase the solid angle of the detector over which adjacent radiation sources (and background) reach the detector.

4.4.3. Pipe Thickness

Attenuation due to the pipe wall thickness determines the transmission of the 185.7 keV gamma rays reaching the detector. Correcting for pipe wall thickness also aids in correlating the density, concentration, and enrichment with measured detector data. Values of 304L stainless steel thickness fall within (0.52±0.05) cm. Using the ISOCS Uncertainty Estimator, the 185.7 keV peak efficiency was determined within the range of (0.52±0.05) cm and plotted in Figure 11. In practice, a section of pipe wall might be considered to be an integral part of the detector and/or wall thickness measured *in-situ*.

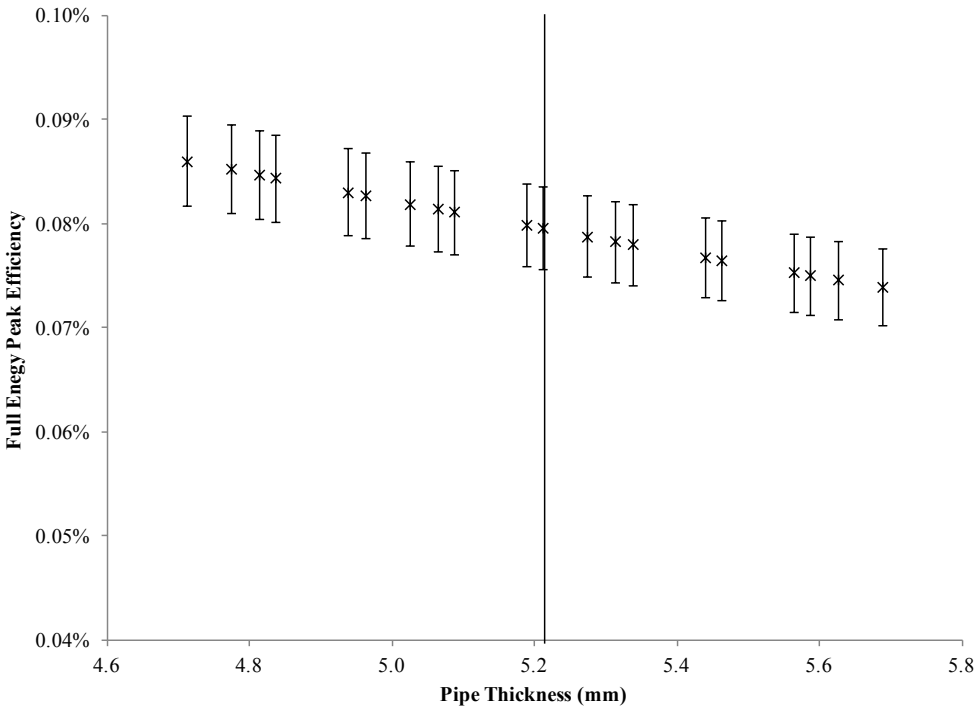

Figure 11. ISOCS Uncertainty Estimator Simulations: Efficiency Calculations for Falcon Detector at Various Pipe Thickness Values.

The linear attenuation coefficient at this energy through 304L pipe was calculated using the *NIST XCOM: Photon Cross Sections Database* (total without coherent scattering) to be 1.14 cm^{-1} with a 55.4% transmission through 0.52 cm of stainless steel [20]. Figure 11 shows the peak efficiency compared to a relative thickness from 0.52 cm.

At the lower end at 0.47 cm, the efficiency increases by 8% (relative to the full energy peak efficiency at the expectation value of the pipe thickness), whereas at the higher end at 0.57 cm, the efficiency drops by 7% (rel.). This pipe range represents a sampling of Schedule 40 304L stainless steel pipe available in industrial production [22] [23]. The result of the detection capability for safeguards monitoring becomes pivotal given a potential 0.1–10% variation in throughput (dependent on plant size) as safeguards criteria. In the absence of an empty pipe calibration, even minute variations in pipe thickness become augmented for monitoring low-energy ^{235}U emissions for safeguards process monitoring.

5. DISCUSSION

The peak efficiency is a combination of factors from the source-detector geometry, source self-absorption, shielding and absorbers, and intrinsic detection efficiency. As a result, these four factors' uncertainty contributes to the overall efficiency of the assay system.

Efficiency values for a high-resolution gamma-ray detector were calculated for the 185.7 keV peak from a combination of measurement data and ISOCS models. For the collimated Falcon BEGe, the dilution measurement data yielded a 185.7 keV peak efficiency of (0.073±0.001)%, where the ISOCS yielded (0.080±0.004. In investigating the effects of each of the four variables ($\varepsilon_{geom} \cdot \varepsilon_{absp} \cdot \varepsilon_{sample} \cdot \varepsilon_{int}$), the ε_{sample} was determined to be (40.2±0.2)% for the Falcon [1], resulting in a *CF(AT)* of 2.49, and κ of ~0.75 in Parker's method in determination of self-attenuation effects.

To put the required level of accuracy in monitoring uranyl nitrate in perspective, the UNCLE is capable of reaching pump speeds of 1700 RPM, which translates approximately into 12,800 kg/h if run at full capacity. Since uranium comprises 8.02% of the uranyl nitrate, the maximal uranium throughput for UNCLE is ~9200 MTU/yr., potentially classifying UNCLE as a large-scale throughput facility. At the tested pump speeds of 500 RPM and 1070 RPM, where the latter speed emulated the throughput of the Springfields conversion facility at 90g U/L, these translate into an annual throughput of 2537 MTU and 5724 MTU at full capacity [10]. Detection of 10 MTU for 1070 RPM equates to a measurement uncertainty no greater than 0.17% [10].

The sensitivity analysis using ISOCS's Uncertainty Estimator provided an indication of how pipe thickness and source-detector distance and offset variables affected the overall efficiency for the modeled Falcon detector. Although the offset measurements varied exponentially as a function of offset distance and source-detector varied as the modified square of inverse of source-detector detector distance, such issues are remedied with effective shielding, sufficiently encasing the detector. The pipe thickness attenuation most affected the 185.7 keV signature peak efficiency by up to 8% for ±0.5 mm changes in Schedule 40 304L stainless steel piping employed in UNCLE. The result of detection capability for safeguards monitoring becomes pivotal given the SQ detection limit for facilities with high uranium throughput. Even minute variations in pipe thickness become augmented for monitoring low-energy ^{235}U emissions for process monitoring, which affect the confidence of safeguards conclusions.

From the data provided in the sensitivity analysis, the pipe thickness was the most prominent variable. With a change of 0.5 mm in pipe thickness, the detection efficiency decreases by up to 8% in the case of the Falcon at 90 g U/L, as calculated by ISOCS. The addition of 0.5 mm of stainless steel thickness decreases the 185.7 keV peak efficiency of the Falcon from 0.080% to 0.074%. Consequently, 8% of the UNCLE annual throughput is ~458 MTU, which is much greater than the IAEA requirement of 10 MTU. Even changing the pipe thickness by ~0.1mm decreases the aforementioned peak efficiency to 0.078%. This 2.5% decrease in efficiency equates a difference of 143.1 MTU/yr., still in ample excess of the IAEA. Consequently, the utmost smallest modification in pipe specification is enough to spoof detected NDA signatures to produce enough variation to divert a much greater quantity than 1 SQ. All defined detector locations and shielding arrangements must be maintained tamper-proof. As seen with existing in-line process monitoring devices, such as the Online Enrichment Monitor (OLEM) [24], such devices can be designed to be enclosed, tamper-indicating (e.g. tamper indicating paint) and under the IAEA's seal. The OLEM system includes multiple redundancy components and can operate on battery power, ensuring reliability and autonomy. All system components are contained in sealed boxes and connected by special tubing, for which all enclosures remain under IAEA seal.

Furthermore, in the scope of this work, only ^{235}U signatures were considered for gamma-ray monitoring. Given that the solution used in the validation experiment was ~40 years old, it was reasonable to assume that conversion facilities (e.g. Springfields) could not be circulating such aged uranyl nitrate; however, it is possible that such facilities could have material in secular equilibrium, warranting investigation of ^{238}U signatures, which would be an appropriate scope for further investigation in this work.

6. CONCLUSIONS

In the context of recent IAEA policy recommendations for monitoring purified compounds in uranium conversion facilities, the scope of this project addressed instrumentation testing in dilution measurements and at ORNL's

UNCLE facility. The objective of this work was to determine the capabilities of passive gamma-ray systems for PM in NUCPs and whether it was possible to meet the IAEA safeguards criteria of detecting 1 SQ (10 MTU) in a time frame of 1 year with a 50% probability of detection. The KMP interpreted as first satisfying INFCIRC/153 Para. 34(C) materials occurred following solvent extraction, producing uranyl nitrate during the conversion process. Based on in-depth experimental measurements, simulations, and uncertainty/sensitivity quantification, the abilities of COTS gamma-ray detectors were evaluated to determine their role in an overall safeguards system to determine if IAEA safeguards criteria could be met.

In the scope of this sensitivity analysis, determining the detector response, through calculation of full energy peak efficiency of the 185.7 keV ^{235}U emission, quantifies the effects of self-attenuation (ε_{sample}), detector position i.e. offset, source-distance (ε_{geom}), and pipe thickness and collimation (ε_{absp}) on each of the four efficiency variables. Experimental data was used with validated ISOCS and MCNPX computational models to determine the sensitivity to each of these variables. Consequently, pipe thickness was the most sensitive variable in affecting full energy peak efficiency. Furthermore, computation of *CF(AT)* (i.e. ε_{sample}) using Parker's method with the approximation $\kappa \approx \pi/4$ was validated through experimental, MCNPX and ISOCS for a uranyl nitrate filled transfer pipe segment. Quantifying sensitivity in detector position becomes increasingly important as considerations from (static) design-scale measurements translate into (dynamic) field operations tests. Notably, voiding effects due to bubbly flow or laminar flow with an air gap in the uranyl nitrate, becomes increasingly important translating to operating conditions, and warrant further investigation.

Although the IAEA requirement of 1 SQ (10 MTU) in a period of 1 year cannot be detected using stand-alone passive gamma measurements, consideration must be given to estimations of how 5 MTU is all that is required to produce 1 SQ of centrifuge material [25]. For NUCPs classified as small (~100 MTU/yr.), 1 SQ represents ~ 10% of the plant throughput. At these levels, it is possible to detect misuse. However, considering the implementation of this criterion in such facilities as those in large (~10,000 MTU/yr.), diversion of 1 SQ becomes essentially undetectable given the systematic uncertainty. Given that the UNCLE facility is capable of circulating uranyl nitrate at the level of a large throughput facility, and given its extremely modest size, consideration must be given to how easily operational design and minor variations in source-detector setup can easily be interpreted as reasonable uncertainty without distinction from the production of undeclared uranyl nitrate.

Acknowledgements

The authors thank Denise Lee, Jeff Chapman, Robert McElroy Jr., Steve Cleveland, Ron Boyd, Chris Pickett, Tyler Guzzardo, Ram Venkataraman, and Joseph Birdwell for their assistance in facilitating this project in various capacities.

Funding

This work was supported by the National Nuclear Security Administration's Office of International Safeguards - Standards and Technology Development and Human Capital Development subprograms.

References

[1] S.A. Dewji, Safeguards assessment of gamma-ray detection for process monitoring at natural uranium conversion facilities, Nuclear and Radiological Engineering Program, Department of Mechanical Engineering, Georgia Institute of Technology, Atlanta, 2014.

[2] International Atomic Energy Agency, Safeguards Measures Applicable in Conversion Plants Processing Natural Uranium (Policy Paper 18), 2003.

[3] International Atomic Energy Agency, The Structure and Content of Agreements between the Agency and States Required in Connection with the Treaty on the Non-Proliferation of Nuclear Weapons, in: International Atomic Energy Agency (Ed.) INFCIRC 153 (corrected), 1972.

[4] International Atomic Energy Agency, IAEA Safeguards Glossary, in: International Atomic Energy Agency (Ed.) International Nuclear Verification Series, Austria, 2001.

[5] B.D. Boyer, D.M. Gordon, L.G. Fishbone, J.R. Lemley, International Safeguards Approach for Uranium Ore Concentrates to Uranium Hexafluoride Conversion Plants, 45th Annual Meeting of the Institute of Nuclear Materials Management (INMM), Orlando, FL, 2004.

[6] R.L. Faulkner, J.M. Begovich, J.J. Ferrada, R.D. Spence, J.M. Whitaker, W.J. Bicha, L.G. Loden, Oak Ridge Efforts to Enhance Conversion Plant Safeguards, 45th Annual Meeting of the Institute of Nuclear Materials Management (INMM), Orlando, FL, 2004.

[7] S.A. Dewji, J.A. Chapman, D. Lee, E.B. Rauch, N.E. Hertel, Use of the UNCLE Facility to Assess Integrated Online Monitoring Systems for Detection of Diversion at Uranium Conversion Facilities, 52nd Annual Meeting of the Institute of Nuclear Materials Management (INMM), Palm Desert, CA, 2011.

[8] S.A. Dewji, R. McElroy, D. Lee, J.A. Chapman, N.E. Hertel, Detector Validation and Source Term Analysis of Uranyl Nitrate to Detect Diversion at Natural Uranium Conversion Facilities, 53rd Annual Meeting of the Institute of Nuclear Materials Management (INMM), Orlando, FL, 2012.

[9] S.A. Dewji, D. Lee, S. Croft, R. McElroy, N.E. Hertel, J.A. Chapman, S. Cleveland, Development of Integrated Online Monitoring Systems for Detection of Diversion at Natural Uranium Conversion Facilities, 54th Annual Meeting of the Institute of Nuclear Materials Management (INMM), Palm Desert, CA, 2013.

[10] S.A. Dewji, D.L. Lee, S. Croft, N.E. Hertel, J.A. Chapman, R. McElroy, S. Cleveland, Validation of gamma-ray detection techniques for safeguards monitoring at natural uranium conversion facilities, Nuclear Instruments and Methods in Physics Research Section A: Accelerators, Spectrometers, Detectors and Associated Equipment, 823 (2016) 135-148.

[11] Canberra Industries Inc., In Situ Gamma Spectroscopy with ISOCS, an In Situ Object Counting System, 2008.

[12] Los Alamos National Laboratory, MCNPX User's Manual - Version 2.6.0, in: D.B. Pelowitz (Ed.), Los Alamos National Laboratory, Los Alamos, NM, 2008.

[13] S.K. Smith, M. Lucas, Gamma-Ray Detectors, in: D. Reilly, N. Ensslin, H. Smith Jr., S. Kreiner (Eds.) Passive Nondestructive Assay of Nuclear Materials, Los Alamos National Laboratory/U.S. Nuclear Regulatory Commission, Washington, 1991.

[14] J.L. Parker, Use of Calibration Standards and the Correction for Sample Self-Attenuation in Gamma-Ray Nondestructive Assay, Los Alamos National Laboratory, Los Alamos, 1984.

[15] S.A. Philips, S. Croft, In-line Monitoring of Radium Slurry by Gamma-Ray Spectrometry, 10th International Conference on Environmental Remediation and Radioactive Waste Management, Glasgow, Scotland, 2005.

[16] K.E. Morris, S.K. Smith, S. Gailey, D.R. Nakazawa, R. Venkataraman, Segmented Gamma Scanner for Small Containers of Uranium Processing Waste- 12295, Waste Management 2012 Phoenix, AZ, 2012.

[17] R. Venkataraman, E-mail Personal Communication: Falcon and ISOCS, in: S.A. Dewji (Ed.), 2013.
[18] S.Y.F. Chu, L.P. Ekström, R.B. Firestone, The Lund/LBNL Nuclear Data Search, 1999.
[19] Canberra Industries, Genie 2000 Gamma Analysis Software, Canberra Industries, 2004.
[20] M.J. Berger, J.H. Hubbell, S.M. Seltzer, J. Chang, J.S. Coursey, R. Sukumar, D.S. Zucker, K. Olsen, XCOM: Photon Cross Sections Database, National Institute of Standards and Technology, 2011.
[21] J.L. Parker, Attenuation Correction Procedures, in: Los Alamos National Laboratory (Ed.) Passive Nondestructive Assay of Nuclear Materials: Attenuation Correction Procedures, U.S. Nuclear Regulatory Commission Office of Nuclear Regulatory Research, 1991.
[22] Onlinemetals.com, Schedule 40 Stainless Steel Pipe T-304/304L, 2013.
[23] Ace Stainless Supply, Schedule 40 - 304L - Pipe, 2013.
[24] International Atomic Energy Agency, New IAEA Uranium Enrichment Monitor to Verify Iran's Commitments under JCPOA, in: International Atomic Energy Agency (Ed.), 2016.
[25] D. Nusbaum, Z. Karpas, Y. Sadan, G. Reich, J. Bedell, S. LaMont, J. Phillips, G. R., Strengthening Safeguards in the Nuclear Fuel Cycle: 1. Diversion Scenarios in the Nuclear Fuel Cycle, 8th International Conference on Facility Operations – Safeguards Interface, Portland, OR, 2008.